Molten Salt Synthesis of $Sr_2Bi_4Ti_5O_{18}$ for Rhodamine B Removal via Adsorption-Photocatalysis Effect

Anton Prasetyo[1*], Syilfia Ainur Rohmah Bashofi[1], Widiya Nur Safitri[2], Arie Hardian[3]

[1]Department of Chemistry, Faculty of Science and Technology, Universitas Islam Negeri Maulana Malik Ibrahim Malang, Jalan Gajayana 50, Malang, 65144, Indonesia

[2]Department of Chemistry, Faculty of Science and Data Analytics, Institut Teknologi Sepuluh Nopember, Keputih, Sukolilo, Surabaya 60111, East Java, Indonesia

[3]Department of Chemistry, Faculty of Sciences and Informatics, Universitas Jenderal Achmad Yani, Cimahi 40531, West Java, Indonesia.

[*]Email: anton@kim.uin-malang.ac.id

Received 25 March 2025
Accepted 24 July 2025
Published 12 December 2025

Abstract

The textile industry's rapid growth has increased dye waste; therefore, effective treatment solutions are needed. Photocatalysis technology has emerged as a promising approach due to its efficiency and environmentally friendly properties. Aurivillius-structured compounds have shown potential as photocatalysts because their ferroelectric properties can inhibit recombinant rate electron-hole. In this research, we synthesized $Sr_2Bi_4Ti_5O_{18}$ (one of the five-layer Aurivillius compound classes) using the molten salt method. Then, we tested its application for adsorption-photocatalysis degradation of rhodamine B. The diffractogram showed that the $Sr_2Bi_4Ti_5O_{18}$ phase was successfully synthesized with minor impurities (Bi_2O_3 and TiO_2) attributed to incomplete reaction processes. The SEM image showed plate-like particles with non-uniform particle sizes was obtained. The Kubelka-Munk result showed that the band gap energy of $Sr_2Bi_4Ti_5O_{18}$ is 3.27 eV. Adsorption tests demonstrated that $Sr_2Bi_4Ti_5O_{18}$ reduced rhodamine B concentration by 52.5% for 30 minutes, which corresponds to its good adsorption capability. Further adsorption-photocatalysis experiments under light exposure showed ~60% reduction in rhodamine B concentration for 60 minutes. The comparison between adsorption and photocatalysis results suggests that adsorption dominates in decreasing rhodamine B concentration. This is likely due to the large number of rhodamine B molecules adsorbed on the surface of $Sr_2Bi_4Ti_5O_{18}$, which prevents light from reaching the $Sr_2Bi_4Ti_5O_{18}$ surface, thereby hindering the degradation of rhodamine B through the photocatalysis mechanism.

Keywords: *adsorption-photocatalysis, molten salt synthesis, rhodamine B, $Sr_2Bi_4Ti_5O_{18}$*

How to cite

Prasetyo, A., Bashofi, S.A.R., Safitri, W.N., & Hardian, A. (2025). Molten Salt Synthesis of $Sr_2bi_4ti_5o_{18}$ for Rhodamine B Removal via Adsorption-Photocatalysis Effect. *Jurnal Kimia Riset*, *10*(2), 167–177.

Highlights

1. $Sr_2Bi_4Ti_5O_{18}$ was successfully synthesized by molten salt synthesis but still found impurities
2. Molten salt synthesis can produce plate-like $Sr_2Bi_4Ti_5O_{18}$ particle
3. $Sr_2Bi_4Ti_5O_{18}$ can adsorp methylene blue
4. The adsorption properties of $Sr_2Bi_4Ti_5O_{18}$ influence to its photocatalysis activity

Introduction

The rapid growth of the textile industry has also led to an increase in the concentration of dye waste produced. Therefore, efforts are needed to address this issue (Berradi et al., 2019). Many Researchers have reported the potential of photocatalysis technology to degrade dyes, offering various advantages, including non-hazardous waste output and greater efficiency in using chemicals and energy (Khan et al., 2024). The photocatalysis mechanism involves converting light energy into chemical energy, which produces hydroxyl radicals that undergo redox reactions with organic compounds (pollutants), and then leading to the degradation of the organic molecules (Khan et al., 2023; Karunamoorthy et al., 2018).

One class of compounds reported to have potential as photocatalyst materials is Aurivillius-structured compounds (Collu et al., 2018; Wang et al., 2020). Aurivillius-structured compounds have the general formula $Bi_2A_{n-1}B_nO_{3n+3}$, composed of $[Bi_2O_2]^{2+}$ layers and perovskite layers with the composition $[A_{n-1}B_nO_{3n+3}]^{2-}$. The *A*-site cation is occupied by large cations such as Na^+, K^+, Ca^{2+}, Sr^{2+}, Ba^{2+}, Pb^{2+}, or Bi^{3+}, while the *B*-site cation is occupied by smaller cations such as Fe^{3+}, Mn^{3+}, Cr^{3+}, Ti^{4+}, Nb^{5+}, or W^{6+}. The integer "*n*" (1, 2, 3...) represents the number of pseudo-perovskite structure layers (Aurivillius, 1949). Thus, the classification of Aurivillius compounds is based on the number of pseudo-perovskite structure layers (*n*). In addition. One of the main properties of Aurivillius compounds is ferroelectricity (Petrovic and Bobic, 2018).

The ferroelectric property is reported to suppress the electron-hole recombination rate, thereby enhancing photocatalytic activity (Khan et al., 2016). Therefore, the utilization of ferroelectric compounds in photocatalytic technology becomes an interesting prospect. In addition, electrons in the O 2*p* and Bi 6*s* orbitals at valence band electronic structures in Aurivillius compounds have also been reported can enhance their photocatalytic activity (Chen et al., 2020). Some Aurivillius compounds that exhibit photocatalytic properties include $Bi_4Ti_3O_{12}$, $SrBi_4Ti_4O_{15}$, and $CaBi_4Ti_4O_{15}$ (Bashofi and Prasetyo, 2022; Kumar and Vaish, 2024; Tu et al., 2019; Al-Abror et al., 2022). $Sr_2Bi_4Ti_5O_{18}$ is one of the members of the five-layer Aurivillius compounds that was reported have photocatalyst activity. Elayaperumal and Malathi (2016) reported that $Sr_2Bi_4Ti_5O_{18}$ has a bandgap energy of 3.34 eV. On other hand, Shi et al. (2023) reported the photocatalytic activity of $Sr_2Bi_4Ti_5O_{18}$, which reduced the concentration of rhodamine B by 99% over 180 minutes. It indicates that the compounds $Sr_2Bi_4Ti_5O_{18}$ have the potential to be used for the treatment of dye wastewater.

The mechanism of organic compound degradation by photocatalytic compounds involves two main stages: adsorption and degradation. The detailed mechanism can be explained as follows: (1) Transfer of organic molecules from the liquid phase to the surface of the photocatalyst. (2) Organic molecules adsorption on the surface of the photocatalyst. (3) The adsorbed molecules undergo a reaction. (4) The reaction produces smaller molecules, and (5) Removal of the products from the photocatalyst surface (Bai et al., 2022). On the other hand, many researchers reported that the synergistic of adsorption-photocatalysis has excellent capability for organic compound removal (Chen et al., 2019). Banerjee, et al. (2021) reported that the synergistic effect of adsorption-photocatalysis in $La_2Ce_2O_7$ material could significantly reduce dye concentrations. It indicates that the synergistic effect of adsorption-photocatalysis offers a promising approach for dye reduction methods with excellent performance. However, studies on the adsorption-photocatalysis properties of Aurivillius compounds are

still very limited, making it urgent to research these properties.

The morphology and particle size material influence the performance of the adsorption-photocatalysis process (Hendrix, et al., 2023). Many researchers have reported that Aurivillius compounds with plate-like morphology exhibit good activity capabilities (Collu et al., 2022). The plate-like Aurivillius compounds with photocatalytic activity include $Bi_4Ti_3O_{12}$, $SrBi_2Ta_2O_9$, and $Bi_6Ti_3WO_{18}$ (Chen et al., 2016; Khodabakhsh et al., 2023; Mi et al., 2018). Meanwhile, the synthesis method reported to produce plate-like Aurivillius compounds successfully is the molten salt method (Ma et al., 2022; Prasetyo et al., 2022). It indicates that the molten salt synthesis method can potentially synthesize high-performance Aurivillius photocatalyst compounds. The synthesis of the $Sr_2Bi_4Ti_5O_{18}$ compound using the molten salt method is still limited. Several researchers have synthesized $Sr_2Bi_4Ti_5O_{18}$ using different methods: (a) Rao et al., (2024) reported the synthesis of $Sr_2Bi_4Ti_5O_{18}$ using the sol-gel method, resulting in micro flower-shaped particles; (b) Shi et al., (2023) synthesized $Sr_2Bi_4Ti_5O_{18}$ using the hydrothermal method, producing plate-like particles, although a significant amount of particle agglomeration was still observed.

Therefore, in this study, $Sr_2Bi_4Ti_5O_{18}$ compounds were synthesized using the molten salt method. The obtained compounds were characterized using (a) XRD, (b) SEM, and (c) UV-Vis DRS. Then, adsorption-photocatalysis tests were studied for rhodamine B removal.

Research Methods

Materials

The chemicals used in this study are: TiO_2 (Sigma Aldrich, 99.9% powder), Bi_2O_3 (Sigma Aldrich, 99.9% powder), $SrCO_3$ (Sigma Aldrich, 99.9% powder), NaCl (Merck, 99.9% powder), KCl (Merck, 99.9% powder), $AgNO_3$ (Merck, powder), acetone (Merck).

Instrumentation

The instrumentation used for the samples obtained characterization are: (a) *X*-ray diffractometer (Rigaku Miniflex diffractometer) (b) Scanning electron microscopy (JEOL JSM-6360LA type), (c) Ultraviolet-visible (UV-Vis) diffuse reflectance spectroscopy (DRS) (Thermo Scientific Evolution 220 spectrometer type).

Procedure

The methods used in this research include synthesis, characterization, and testing of adsorption-photocatalysis properties in reducing the concentration of rhodamine B.

1) Synthesis

The synthesis of $Sr_2Bi_4Ti_5O_{18}$ compounds was carried out using the molten salt method. The precursors were weighed stoichiometrically with a target compound mass of 4 grams. The synthesis of the compounds was carried out using the molten salt method. It used mixed salt of NaCl/KCl with a molar ratio of 1:1, and the molar ratio of the target compound to the salt was 1:7. The mixture of precursors and salt was ground in an agate mortar for 1 hour, and acetone was added to achieve better homogeneity. The precursor and salt mixture was then calcined at 675, 775, and 825°C for 6 hours. Then, the product was washed with hot deionized water to remove the salt content. The presence of salt residue was identified using an $AgNO_3$ solution. And then, the salt-free samples were dried in an oven at 100°C for 4 hours.

2) Characterization

The characterization techniques used for the samples are: (a) *X*-ray diffraction technique to determine the phases of the formed compounds with a measurement range: 2θ (°) = 3-90 (b) Scanning electron microscopy to

observe the morphology and particle size distribution, and (c) Ultraviolet-visible (UV-Vis) diffuse reflectance spectroscopy (DRS) to calculate the band gap energy. The energy band gap calculation for $Sr_2Bi_4Ti_5O_{18}$ uses indirect band gap model (Wang et al., 2020).

3) Adsorption-Photocatalysis Test

The testing was conducted using a homemade photoreactor with dimensions of 40×40×40 cm and used 1 lamp UV Commercial (commercial LED UV Spotlight Bulb 80 LEDs 220V E27). A 100 mL solution of 4 ppm rhodamine B was mixed with 100 mg of $Sr_2Bi_4Ti_5O_{18}$ and placed in a beaker glass, which was then put inside the photoreactor. The adsorption test was performed for 30 minutes without UV light exposure, while the adsorption-photocatalysis test was conducted for 60 minutes under UV light exposure. After the tests were completed, the solution was filtered to separate the catalyst, and the filtrate was analyzed using UV-Vis spectroscopy to determine the remaining concentration of rhodamine B (Bashofi et al., 2023).

Results and Discussion

The diffractogram of the $Sr_2Bi_4Ti_5O_{18}$ compound is shown in Figure 1 and compared with the standard $Sr_2Bi_4Ti_5O_{18}$ data (ICSD number 150401). The comparison results show a match that indicates the target $Sr_2Bi_4Ti_5O_{18}$ compound has been formed. The characteristic peaks of the $Sr_2Bi_4Ti_5O_{18}$ compound were found at the 2θ (°): 21.96, 23.44, 32.66, 33.12, 47.42, 48.46, 52.24, 53.3, 57.42, and 63.32. The *X*-ray diffraction pattern also reveals additional peaks that indicate the presence of impurities, namely (a) Bi_2O_3 (16.24°); and (b) TiO_2 brookite (48°). The presence of these precursors indicates that the reaction has not been completed perfectly. The low intensity of the impurity peaks also indicates that the impurity concentration is very small, suggesting that technical factors, such as non-homogeneous grinding may lead to the appearance of impurities.

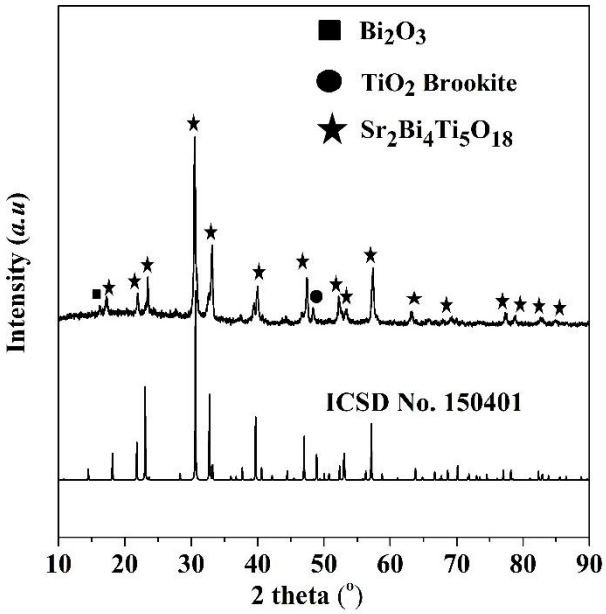

Figure 1. The diffractogram of $Sr_2Bi_4Ti_5O_{18}$

SEM image of $Sr_2Bi_4Ti_5O_{18}$ is shown in Figure 2, and it can be observed that the particle shape is plate-like with non-uniform sizes, and small agglomerated particles are still present. The plate-like particle is a characteristic morphology of Aurivillius compounds reported by many previous researchers (Zhao et al., 2014). The results of the particle distribution measurement (Figure 3) also indicate that the particle size of $Sr_2Bi_4Ti_5O_{18}$ is 1–5 µm. The growth mechanism of plate-like Aurivillius particles was proposed by Zhao et al., (2014), involving two main stages: (a) nucleation and (b) crystal growth. The particle size distribution analysis shows that the obtained particles are relatively large, indicating that the crystal growth stage is more dominant (Prasetyo et al., 2022).

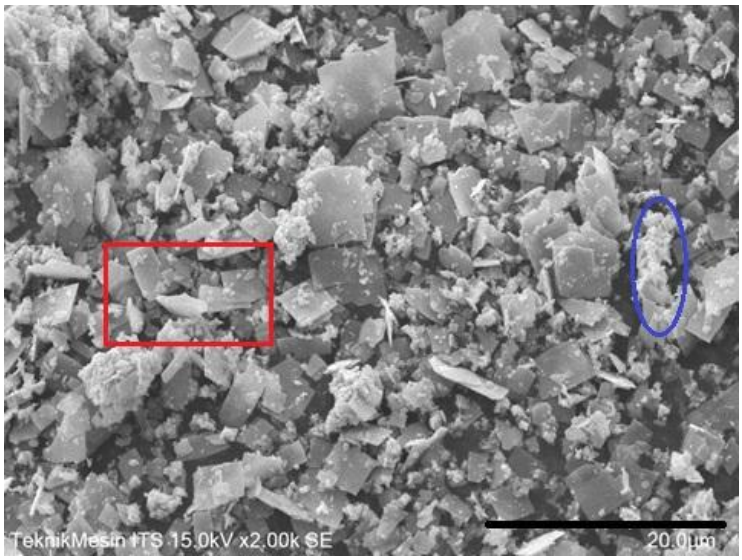

Figure 2. SEM image of $Sr_2Bi_4Ti_5O_{18}$ (The red box is an example of a plate-like particle and the blue oval is an example of an agglomerated particle)

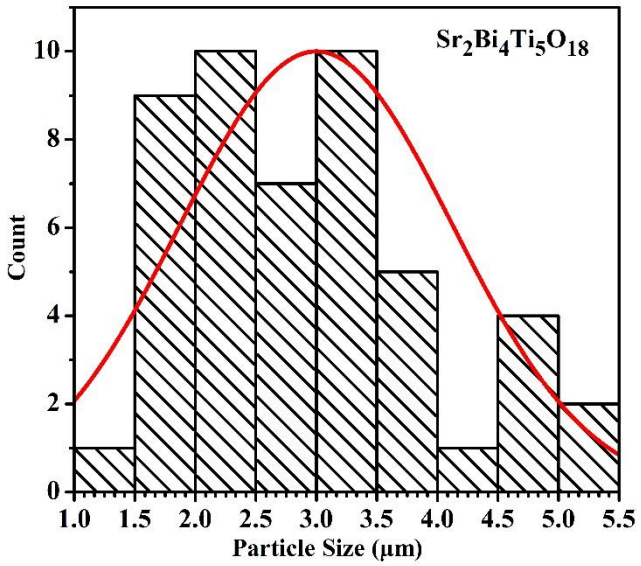

Figure 3. Particle size distribution

The calculation result using Kubelka-Munk (Tauc plot) is shown in Figure 4, and it can be seen that the band gap energy of $Sr_2Bi_4Ti_5O_{18}$ is 3.27 eV. The obtained band gap energy value is almost the same as that reported by many previous researchers. The electronic transition involves conduction band (CB) electrons

in the O 2*p* + Bi 6*s* orbitals moving to the valence band (VB) in the Ti 3*d* orbital (Tu et al., 2019; Rao et al., 2024). The band gap energy value also indicates that the $Sr_2Bi_4Ti_5O_{18}$ photocatalyst material requires excitation source (lamp) with a wavelength of 379 nm (UV light region).

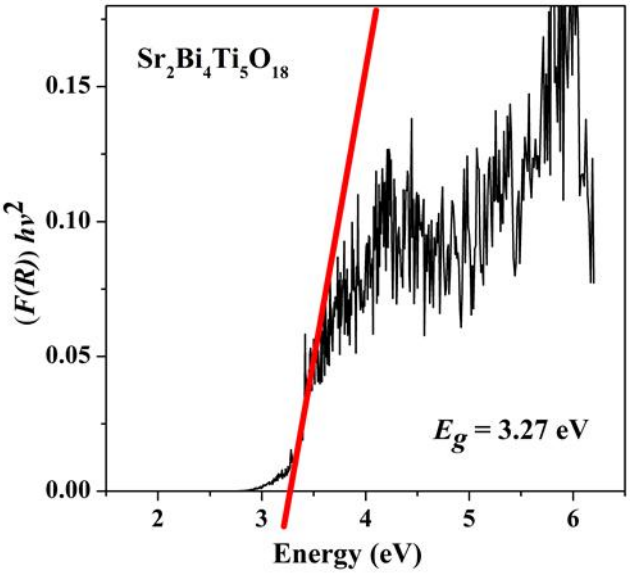

Figure 4. Plot Tauc of $Sr_2Bi_4Ti_5O_{18}$

The test results for the ability of the $Sr_2Bi_4Ti_5O_{18}$ compound to adsorb rhodamine B (adsorption capability) are shown in Figure 5. The test results indicate that the $Sr_2Bi_4Ti_5O_{18}$ compound has good adsorption capability. $Sr_2Bi_4Ti_5O_{18}$ can reduce the concentration of ciprofloxacin by 52.5% within 30 minutes. Aurivillius compounds have been reported to exhibit adsorption properties. Al-Abror et al. (2022) reported that the four-layer Aurivillius compound $SrBi_4Ti_4O_{15}$ can absorb methylene blue. Ziyadiini et al. (2021) also reported that Co-doped $SrBi_4Ti_4O_{15}$ could adsorb rhodamine B through chemical adsorption. The study of adsorption properties in Aurivillius compounds is still very limited. However, by adopting the adsorption model of the perovskite structure, it can be assumed that the adsorption ability of Aurivillius compounds involves interactions between Sr-O bonds and rhodamine B (Luu et al., 2016). The good adsorption properties of Aurivillius compounds offer advantages for their photocatalytic applications. The degradation mechanism in photocatalysis, which involves several stages: (1) the transfer of molecules from the liquid phase to the photocatalyst material surface (solid phase), (2) adsorption on the photocatalyst material surface, (3) degradation reactions on the photocatalyst material surface, and (4) desorption of degradation products (Bai et al., 2022). It indicated that the adsorption properties of $Sr_2Bi_4Ti_5O_{18}$ influenced its photocatalytic performance.

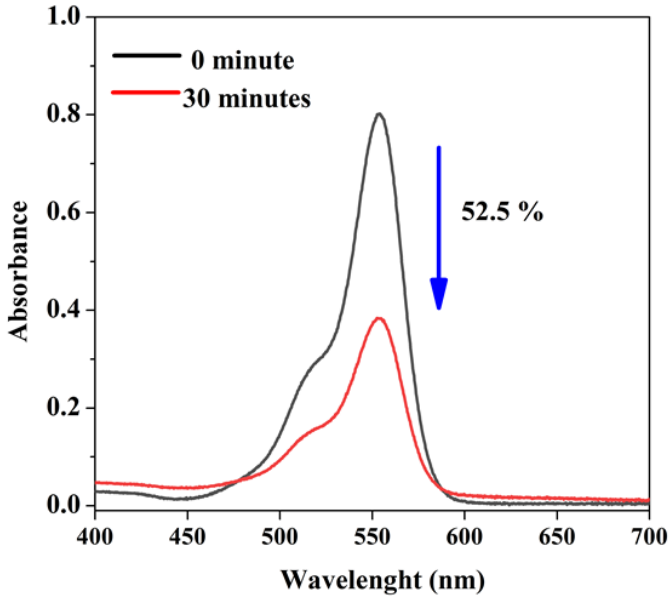

Figure 5. Adsorption test (The blue arrow indicates the percentage decrease in rodhamine B concentration)

The results of the adsorption-photocatalysis test (under light exposure) are shown in Figure 6, and it can be observed that the concentration of rhodamine B decreased by approximately 60% within 60 minutes. The test results obtained are higher than those of the adsorption test alone, indicating that the photocatalyst contributes to the degradation mechanism. Comparing between adsorption and adsorption-photocatalysis results showed that the adsorption process has a greater contribution to the reduction of rhodamine B concentration. The rhodamine B concentration decreases in the adsorption-photocatalyst experiment was not significantly different from the result in the adsorption experiment. This may be due to the high adsorption properties blocking light from reaching the catalyst surface, thereby hindering the catalytic process from proceeding effectively (Janus et al, 2023; Hikmah and Prasetyo, 2025). The other factor is may be due to the band gap energy of the $Sr_2Bi_4Ti_5O_{18}$ compound, which is 3.27 eV. It showed that the photocatalyst operates with light at a wavelength of 379.15 nm. Meanwhile, in this experiment, a commercial UV lamp was used (the data of wavelength is unkonown), which may have resulted in suboptimal electron excitation from VB to CB.

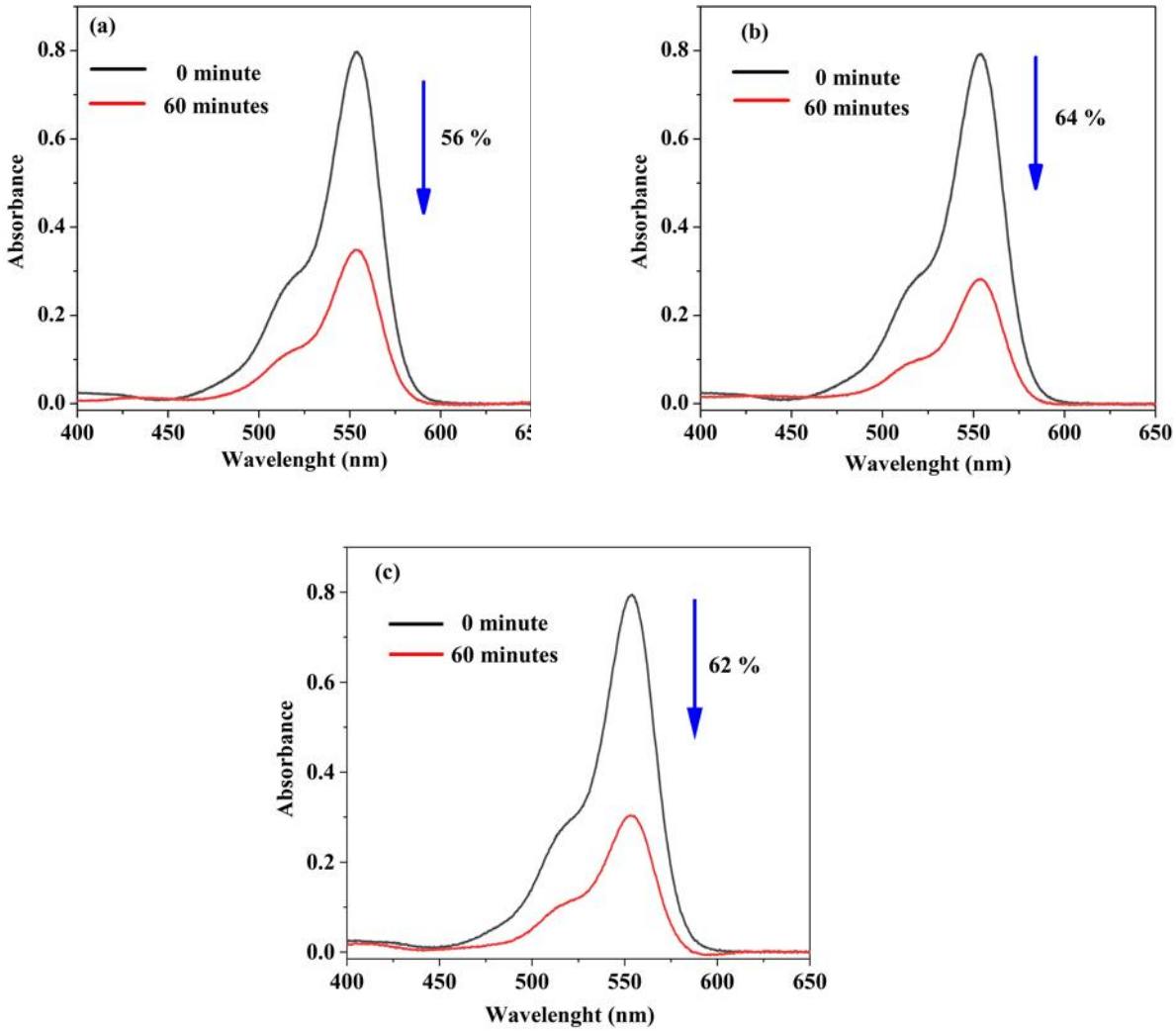

Figure 6. Adsorption-photocatalysis tests: (a) experiment 1, (b) experiment 2, dan (c) experiment (The blue arrow indicates the percentage decrease in Rhodamine B concentration)

Conclusions

The $Sr_2Bi_4Ti_5O_{18}$ compound was successfully synthesized using the molten salt method, although some impurity phases (Bi_2O_3 and TiO_2 (brookite)) were still detected. SEM images show that the resulting $Sr_2Bi_4Ti_5O_{18}$ particles have a plate-like morphology, while calculations using the Kubelka-Munk equation indicate that this compound has a band gap energy of 3.27 eV. Adsorption tests revealed that the compound exhibits excellent adsorption capability (able to reduce rhodamine B concentration by 52.5% for 30 minutes). However, this property hinders the photocatalytic mechanism, resulting in a reduction in rhodamine B concentration via the adsorption-photocatalysis mechanism that is not significantly different from that of the adsorption mechanism alone.

Author Contribution

AP contributed to (a) the concept as well as design the research (b) data analysis, (c) writing the manuscript. **SARB** contributed to (a) the laboratory work (b) data analysis (c) writing manuscript. **WNS** contributed to SEM image analysis. **AR** contributed to diffractogram analysis.

Conflict of Interest

The authors declare no conflict of interest.

Declaration of Artificial Intelligence (AI)

Artificial intelligence (AI) tools, services, or technologies were not utilised in the preparation, analysis, or editing of this manuscript. All content was entirely prepared, reviewed, and verified by the authors without any AI assistance.

Acknowledgement

We thank's to Department of Chemistry, Faculty Science and Technology, Universitas Islam Negeri Maulana Malik Ibrahim Malang for laboratory facilities

Funding

This research did not involve any funding sources from any institution.

References

Al-Abror, M.L., Hastuti, E., & Prasetyo, A. (2022). Molten Salt Synthesis of Photocatalyst Material $SrBi_4Ti_4O_{15}$ for Methylene Blue Degradation. *Jurnal Rekayasa Kimia & Lingkungan*, *17*(2), 182–189. https://doi.org/10.23955/rkl.v17i2.25288

Aurivillius, B. (1949). Mixed Bismuth Oxides with Layer Lattices. 1. The Structure Type of $CaNb_2Bi_2O_9$. *Arkiv for Kemi*, *1*(54), 463-480.

Bai, X., Chen, W., Wang, B., Sun, T., Wu, B., & Wang, Y. (2022). Photocatalytic Degradation of Some Typical Antibiotics: Recent Advances and Future Outlooks. *International Journal of Molecular Sciences*, *23*(15), 8130. https://doi.org/10.3390/ijms23158130.

Banerjee, S., Debnath, A., Allam, B.K., & Musa, N. (2021). Adsorptive and Photocatalytic Performance of Perovskite Material for the Removal of Food Dye in an Aqueous Solution. *Environmental Challenges, 5*, 100240. https://doi.org/10.1016/j.envc.2021.100240

Bashofi, S.A.R., & Prasetyo, A. (2023). Degradasi Rhodamin B oleh $Bi_4Ti_3O_{12}$ yang diperoleh dari Metode Lelehan Garam Campuran NaCl/KCl. *Positron*, *13*(2), 104-111. https://doi.org/10.26418/positron.v13i2.69085

Berradi, M., Hsissou, R., Khudhair, M., Assouag, M., Cherkaoui, O., El Bachiri, A., & El Harfi, A. (2019). Textile Finishing Dyes and Their Impact on Aquatic Environs. *Heliyon*, *5*(11), e02711. https://doi.org/10.1016/j.heliyon.2019.e02711

Jie Chen, J., Xiong, Y., Duan, M., Li, X., Li, J., Fang, S., Qin, S., & Zhang, R. (2020). Insight into the Synergistic Effect of Adsorption-Photocatalysis for the Removal of Organic Dye Pollutants by Cr-doped ZnO. *Langmuir*, *36*(2), 520-533. https://doi.org/10.1021/acs.langmuir.9b02879

Chen, P., Liu, H., Cui, W., Lee, S.C., Wang, L., & Dong, F. (2020). Bi-based Photocatalysts for Light-Driven Environmental and Energy Applications: Structural Tuning, Reaction Mechanisms, and Challenges: Review. *EcoMat*, *2*, e12047. https://doi.org/10.1002/eom2.12047

Chen, Z., Jiang, H., Jin, W., & Shi, C. (2016). Enhanced Photocatalytic Performance over $Bi_4Ti_3O_{12}$ Nanosheets with Controllable Size and Exposed {001} Facets for Rhodamine B Degradation. *Applied Catalysis B: Environmental*, *180*, 698-706. https://doi.org/10.1016/j.apcatb.2015.07.022

Collu, D. A., Carucci, C., Piludu, M., Parsons, D. F., & Salis, A. (2022).

Aurivillius Oxides Nanosheets-based Photocatalysts for Efficient Oxidation of Malachite Green Dye. *International Journal of Molecular Sciences*, *23*(10), 5422. https://doi.org/10.3390/ijms23105422.

Elayaperumal, E., & Malathi, M. (2016). Effect of CuO Addition on Magnetic and Electrical Properties of $Sr_2Bi_4Ti_5O_{18}$ Lead-free Ferroelectric Ceramics, *Ceramics International*, *42*(5), 5830-5841. https://doi.org/10.1016/j.ceramint.2015.12.126.

Hendrix, Y., Rauwel, E., Nagpal, K., Haddad, R., Estephan, E., Boissière, C., & Rauwel, P. (2023). Revealing the Dependency of Dye Adsorption and Photocatalytic Activity of ZnO Nanoparticles on Their Morphology and Defect States. *Nanomaterials*, *13*, 1998. https://doi.org/10.3390/nano13131998

Hikmah, N., & Prasetyo, A. (2025). Adsorption-Photocatalysis Synergy of $Bi_4Ti_{2.9}Fe_{0.1}O_{12}$ for Ciprofloxacin Removal, *Neutrino*, *17*(2), 81-88. https://doi.org/10.18860/neu.v17i2.31329

Janus, M., Kusiak-Nejman, E., & Morawski, A.W. (2011). Determination of the Photocatalytic Activity of TiO_2 with High Adsorption Capacity. *Reaction Kinetics, Mechanisms and Catalysis*, *103*, 279-288. https://doi.org/10.1007/s11144-011-0326-z

Karunamoorthy, S., & Velluchamy, M. (2018). Design and Synthesis of Bandgap Tailored Porous Ag/NiO Nanocomposite: an Effective Visible Light Active Photocatalyst for Degradation of Organic Pollutants. *Journal of Materials Science: Materials in Electronic*s, *29*, 20367-20382. https://doi.org/10.1007/s10854-018-0172-0.

Khan, M. A., Nadeem, M. A., & Idriss, H. (2016). Ferroelectric Polarization Effect on Surface Chemistry and Photo-Catalytic Activity: a Review. *Surface Science Reports*, *71*(1), 1-31. https://doi.org/10.1016/j.surfrep.2016.01.001.

Khan, K. A., Shah, A., Nisar, J., Haleem, A., & Shah, I. (2023). Photocatalytic Degradation of Food and Juices Dyes via Photocatalytic Nanomaterials Synthesized through Green Synthetic Route: a Systematic Review. *Molecules*, *28*(12), 4600. https://doi.org/10.3390/molecules28124600

Khan, S., Noor, T., Iqbal, N., & Yaqoob, L. (2024). Photocatalytic Dye Degradation from Textile Wastewater: a Review. *ACS Omega*, *9*(20), 21751-21767. https://doi.org/10.1021/acsomega.4c00887

Khodabakhsh, M.R., Yilmaz, B., Firoozi, S., Haghshenas, D.F., & Una, U. (2023). Enhanced Photocatalytic Properties of Restacked Unilamellar $[SrTa_2O_7]^{2-}$ Nanosheets of Aurivillius Phase Layered Perovskites. *ACS Omega*, *8*(11), 10607-10617. https://doi.org/10.1021/acsomega.3c00593

Kumar, P., & Vaish, R. (2024). Effect of Poling on Photocatalytic Activity with $SrBi_4Ti_4O_{15}$ Catalyst. *Journal of the American Ceramic Society*, *107*, 6138-6151. https://doi.org/10.1111/jace.19872

Luu, M.D., Dao, N.N., Nguyen, D.V., Pham, N.C., Vu, T.N., & Doan, T.D. (2016). A New Perovskite-type $NdFeO_3$ Adsorbent: Synthesis, Characterization, and As (V) Adsorption. *Advances in Natural Sciences: Nanoscience and Nanotechnology, 7*, 025015. https://doi.org/10.1088/2043-6262/7/2/025015

Ma, Y., Xie, H., Sun, Y., Kou, Q., Liu, L., Yang, B., Cao, W., Chang, Y., & Li, F. (2022). Topochemical Synthesis and Structural Characteristics of Orientation-Controlled $(Bi_{0.5}Na_{0.5})_{0.94}Ba_{0.06}TiO_3$ Perovskite Microplatelets. *Microstructures*, *2*, 2022006. https://doi.org/10.20517/microstructures.2021.13

Mi, L., Feng, Y., Cao, L. Xue, M., Qin, C., Huang, Y., Qin, L., & Seo, H.J. (2018). Photocatalytic Ability of $Bi_6Ti_3WO_{18}$ Nanoparticles with a Mix-layered Aurivillius structure. *Journal of Nanoparticle Research, 20*, 2. https://doi.org/10.1007/s11051-017-4101-6

Petrovic, M.M.V., & Bobic, J.D. (2018). 2-Perovskite and Aurivillius: Types of Ferroelectric Metal Oxides, Editor(s): Biljana D. Stojanovic, in Metal Oxides, Magnetic, Ferroelectric, and Multiferroic Metal Oxides, *Elsevier*, 35-49. https://doi.org/10.1016/B978-0-12-811180-2.00002-5

Prasetyo, A., Guntur, A.N.M., Himmah, S.N., Aini, N., Rouf, U.A., & Aziz, A. (2022). Synthesis of Microsheets $Bi_4Ti_3O_{12}$, and $Bi_4Ti_{2.95}V_{0.05}O_{12}$ via Molten NaCl-KCl Salt Method. *Journal of Pure & Applied Chemistry Research*, *11*(3), 207-213. https://doi.org/10.21776/ub.jpacr.2022.011.03.703

Rao, Z., Cai, W., Yan, Y., Huang, R., Wang, F., Wang, Z., Gao, R., Chen, G., Deng, X., Lei, X., & Fu, C. (2024). Hierarchical Ordered Mesoporous $Sr_2Bi_4Ti_5O_{18}$ Microflowers with Rich Oxygen Vacancies in Situ Assembled by Nanosheets for Piezo-Photocatalysis., *Inorganic Chemistry, 63*(46), 22101-22117. https://doi.org/10.1021/acs.inorgchem.4c03520

Shi, H., Liu, Z., Chen, J. Cui, L., Wang, Z., Luo, Y., & Zhang, J. (2023). Hydrothermal Synthesis of Layered Perovskite $Sr_2Bi_4Ti_5O_{18}$ for Efficient Photocatalytic Degradation of Organic Pollutants. *The Journal of Materials Science*, *58*, 7092-7105. https://doi.org/10.1007/s10853-023-08479-3

Tu, S., Zhang, Y., Reshak, A. H., Auluck, S., Ye, L., Han, X., Ma, T., & Huang, H. (2019). Ferroelectric Polarization Promoted Bulk Charge Separation for Highly Efficient CO_2 Photoreduction of $SrBi_4Ti_4O_{15}$. *Nano Energy*, *56*, 840-850. https://doi.org/10.1016/j.nanoen.2018.12.016

Wang Y, Zhang M, Wu J, Hu Z, Zhang H, & Yan H. (2020). Ferroelectric and Photocatalytic Properties of Aurivillius Phase $Ca_2Bi_4Ti_5O_{18}$. *Journal of the American Ceramic Society, 104*, 322-328. https://doi.org/10.1111/jace.17466

Zhao, Z., Li, X., Ji, H., & Deng, M. (2014). Formation Mechanism of Plate-like $Bi_4Ti_3O_{12}$ Particles in Molten Salt Fluxes, *Integrated Ferroelectrics*, *154*(1), 154-158. https://doi.org/10.1080/10584587.2014.904705

Ziyaadini, M. & Ghashang, M. (2021). Removal of Rhodamine B from Aqueous Solution using $SrCo_xBi_4Ti_{4-x}O_{15}$ Aurivillius Phase Ceramics, *Inorganic and Nano-Metal Chemistry*, *51*(10), 1337-1343. https://doi.org/10.1080/24701556.2020.1835973